Journal of Industrial and Engineering Chemistry 78 (2019) 90–96

Contents lists available at ScienceDirect

Journal of Industrial and Engineering Chemistry

journal homepage: www.elsevier.com/locate/jiec

Optimization of photocatalytic degradation of Cefradine using a "green" goethite/H_2O_2 system

Ruiping Li[a], Shaoming Hong[a], Xiaocong Li[b], Bin Zhang[a], Hailin Tian[a], Yingping Huang[a,*]

[a] Engineering Research Center of Eco-environment in Three Gorges Reservoir Region, Ministry of Education, China Three Gorges University, Yichang 443002, China

[b] Yichang Humanwell Pharmaceutical Co.,Ltd, Yichang 443005, China

ARTICLE INFO

Article history:
Received 7 September 2018
Received in revised form 27 December 2018
Accepted 18 June 2019
Available online 27 June 2019

Keywords:
Goethite
Cefradine
Photocatalytic degradation
Response surface methodology
Box–Behnken Design

ABSTRACT

An environmental friendly photocatalyst, goethite in the presence of H_2O_2, was used to remove Cefradine from aqueous solution. Four factors were examined using Box–Behnken Design and results were analyzed by response surface method. H_2O_2 concentration had the largest effect on Cefradine removal and the optimal reaction conditions were: H_2O_2 concentration, 4 mmol/L; solution pH, 5; goethite dosage, 1.2 g/L and illumination time, 9 h. Experimental data on Cefradine removal under optimal conditions closely coincided with model predictions, validating the model. Hydroxyl radicals (•OH) and superoxide anion were involved in the Cefradine photodegradation process and that •OH makes the larger contribution.

Introduction

Cephalosporins (CEPs) are increasingly the preferred antibiotics for both human diseases and animal infections [1]. The detection frequency of CEPs in aquatic environment is increasing due to their extensive use and, in some cases, overuse [2]. CEPs enter the environment through pharmaceutical manufacturing processes, hospital effluents [3] and industrial farming [4]. Because residual CEPs and metabolites in both water [5–10] and soil [11,12] pose risks to public health and the environment, developing removal methods is important.

Several techniques have been used to eliminate CEPs from water and wastewater, including chlorination [13], oxidation [14–18], adsorption [19–21], photolysis [22–24], and advanced oxidation processes (AOPs) [25–30]. Photocatalytic AOP is a preferred method due to high efficiency and safety. Hydroxyl radicals (•OH) are produced and react with a wide variety of organic pollutants to produce CO_2 and H_2O [31–33]. A few studies have reported on the removal of CEPs by photocatalytic AOP, but either used an expensive catalyst [28,30] or required UV light activation [25–27,29]. Goethite is a promising alternative for CEP degradation as it is abundant, biocompatible and activated by visible light.

Goethite (α-FeOOH) is one of the most thermodynamically stable iron oxides, an abundant mineral frequently found in ores, sediments and soils [34]. Studies on goethite reveal that it can act as a Fenton-like catalyst and photocatalyst. Goethite is not an efficient photocatalyst due to recombination of photogenerated carriers, but H_2O_2 increases catalytic efficiency [34,35]. For example, several authors have reported that the goethite/H_2O_2 system catalyzes the oxidation of methyl orange [36], *p*-chloronitrobenzene [37], 2-chlorophenol [35], and p-nitrophenol [38]. Its application for pharmaceutical degradation of amoxicillin [39] and paracetamol [40] has recently been reported. Goethite is a low cost, efficient photocatalyst for organic pollutant degradation. Further, because goethite is widespread in the soil environment, it has been exploited for in situ remediation of soil and groundwater by adding H_2O_2 to initiate Fenton-like reactions [41].

In this study, Cefradine (CRD), a first generation cephalosporin antibiotic, was selected as the model pollutant. It has been used extensively in human and veterinary medicine because of good activity against gram-positive bacteria [42]. CRD has been detected in a wide range of aqueous matrices [2] and its photolysis products illicit a chronic toxic response in freshwater algae [43]. In 2016, Chen et al. [26] used pure TiO_2 and carbon quantum dots/TiO_2 nanocomposite for photo-degradation of CRD under UV light. CRD removal of 70–75% was achieved in 60 min, at pH 2.85 or pH 9.46. Hydrolysis contributed significantly to CEP removal as the hydrolysis rate is relatively high under acidic or basic conditions [2]. The need for pH adjustment and UV light both limit application

* Corresponding author.
E-mail address: chem_ctgu@126.com (Y. Huang).

https://doi.org/10.1016/j.jiec.2019.06.035
1226-086X/

of this degradation method. This study explores a low-cost, green removal method using the goethite/H_2O_2 system to degrade CEP.

Parameters affecting the photocatalytic efficiency of the goethite/H_2O_2 system include the initial catalyst concentration, solution pH, H_2O_2 concentration and illumination time. A statistical approach, using the response surface methodology (RSM) with a Box–Behnken Design (BBD) was used to analyze the effect of varying each parameter. In this case, a four factorial Box–Behnken Design was used to analyze and optimize the photocatalytic system. The objective of this study was to address three questions about the goethite/H_2O_2 system: (1) How much does each factor contribute to CRD removal? (2) What factor most affects the photodegradation efficiency of CRD? (3) What are the optimal conditions and mechanism for CRD removal.

Materials and methods

Reagents

Cefradine (CRD) was procured from Ehrenstorfer GmbH (99.0%). Acetonitrile and formic acid (HPLC grade) were obtained from Sigma-Aldrich Co., Ltd. Goethite (α-FeOOH, 60.9% Fe) was purchased from Sigma-Aldrich Co. The structure of goethite was confirmed by X-ray diffraction (XRD, D/max 2500, Rigaku, Japan) with Cu–Ka radiation (λ = 1.5406 Å) at room temperature. Morphology and surface properties were observed using a scanning electron microscope (SEM, JSM-7500 F, JEOL, Japan). The UV–vis diffuse reflectance spectrum (UV–vis DRS) was recorded on a Shimadzu UV 3100 spectrophotometer.

Photocatalytic degradation procedures

The photodegradation of CRD in the goethite/H_2O_2 suspension was carried out using a series of 100 mL photo-reaction tubes in an XPA photo-reactor (Xujiang Electromechanical Plant, Nanjing, China) with a 400 W metal halogen lamp (≥420 nm). Each tube received 30 mL of a suspension containing CRD (10 mg/L) and goethite (0.5, 1.0 or 1.5 g/L), with initial pH (5, 6 or 7) adjusted using $HClO_4$ (0.1 mol/L) or NaOH (0.1 mol/L). CRD was set a 10 mg/L because this concentration resulted in appropriate kinetics. Prior to photocatalysis, the suspensions were placed in the dark for 30 min to allow adsorption of CRD by goethite to reach equilibrium. The reaction was initiated by adding H_2O_2 to the reaction mixture and turning on the halogen lamp. To monitor degradation, 1 mL aliquots were removed at specified times, filtered (0.22 μm) and immediately analyzed for CRD. CRD was determined using HPLC-UV (HPLC-1220, Agilent) at 262 nm with a Kromasil C_{18} column (4.6 mm × 250 mm, 5 μm, temperature 30 °C) and a mobile phase consisting of acetonitrile and 0.5% formic acid (18:82, v/v, 1.0 mL/min). All experiments were performed in duplicate.

Table 1
Range and levels of the independent variables used in the BBD model.

Independent variable (unit)	Factor	Level		
		Low (−1)	Medium (0)	High (1)
H_2O_2 concentration (mmol/L)	X_1	1	3	5
pH	X_2	5	6	7
Goethite dosage (g/L)	X_3	0.5	1.0	1.5
Illumination time (h)	X_4	6	8	10

The primary reactive oxygen species (ROS) during photocatalysis was identified by adding selective scavengers to the degradation reaction mixture. Isopropanol (IPA, 10 mmol/L) was added to scavenge the hydroxyl radical ($^{\bullet}OH$) and benzoquinone (BQ, 10 mmol/L) to scavenge the superoxide radical ($O_2^{\bullet-}$).

Response surface design

The Design Expert V.8.0.6 software was applied in the Box–Behnken Design (BBD) of the experiment and performed response surface modeling, statistical analysis and optimization. The experimental design consisted of four independent parameters, each at three levels. The CRD degradation rate (Y) was the response variable, while H_2O_2 concentration (X_1, mmol/L), pH (X_2), goethite dosage (X_3, g/L) and illumination time (X_4, hour) were chosen as the independent variables. CRD degradation was carried out using 29 combinations of the four reaction parameters. The variables and levels of the BBD model are shown in Table 1, with level ranges based on preliminary experiments. Analysis of variance (ANOVA) was used to evaluate the CRD degradation variables. The interactions between the dependent and independent variables can be fitted to a mathematical second-order polynomial model as expressed in Eq. (1):

$$Y = \beta_0 + \sum \beta_i X_i + \sum \beta_{ii} X_i^2 + \sum \beta_{ij} X_i X_j \quad (1)$$

Where, Y = predicted response (CRD degradation rate, %); X_i, X_j = dimensionless coded independent variables; β_0 = model constant coefficient; β_i = linear coefficients, β_{ii} = quadratic coefficients and β_{ij} = interaction coefficients.

Results and discussion

Catalyst characterization

Fig. 1 shows the XRD pattern and SEM image for the goethite used in this study. All XRD peaks matched the standard diffraction

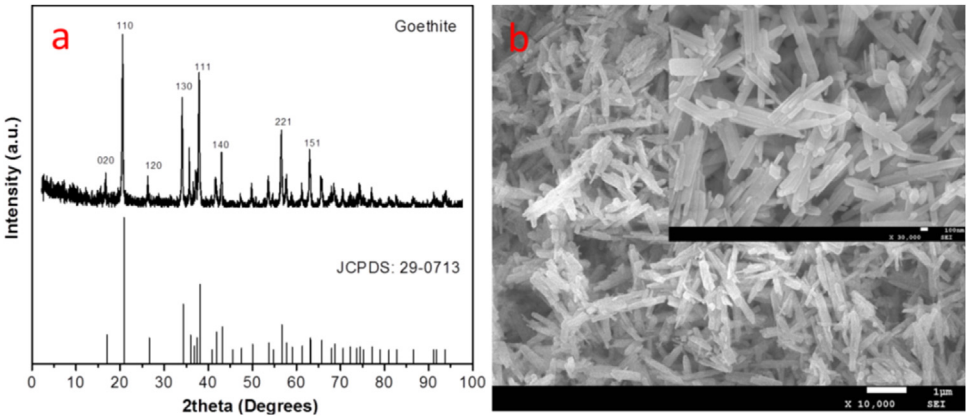

Fig. 1. XRD pattern (a) and SEM image (b) of the investigated goethite.

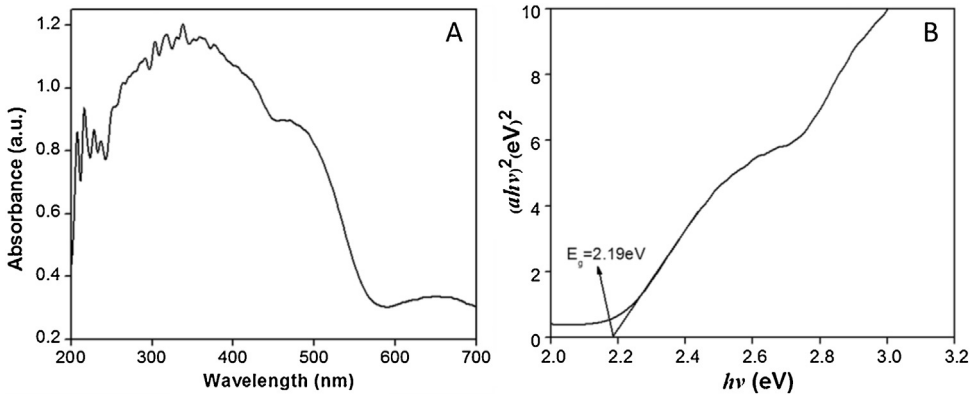

Fig. 2. UV–vis DRS (A) and the according band gap calculated (B) of goethite sample.

data for orthorhombic α-FeOOH (JCPDS No. 29-0713) (Fig. 1a). The SEM image (Fig. 1b) shows the fibrous goethite crystals of length 150–650 nm. The UV–vis diffuse reflectance spectrum of goethite is displayed in Fig. 2a. Goethite absorbs strongly in the ultraviolet and visible (<590 nm) regions. The band-gap energy (E_g) of goethite is 2.19 eV, as obtained from the plot of $(\alpha h\nu)^2$ vs energy ($h\nu$) [44]. The calculated valence (E_{VB}) and conduction (E_{CB}) band edge potentials of goethite are, respectively, 2.98 eV and 0.79 eV vs. NHE [45].

Model fitting and analysis of variance

The BBD design with experimental and predicted results for CRD photocatalytic degradation is given in Table 2. The experiment consisted of 29 runs and an empirical relationship describing the CRD degradation rate as function of the individual and interaction contributions of variables was expressed by the following second-order polynomial equation:

$$Y = 80.18 + 18.12X_1 - 7.46X_2 + 2.91X_3 + 7.12X_4 - 0.55X_1X_2 - 0.72X_1X_3 - 1.07X_1X_4 - 0.57X_2X_3 - 1.10X_2X_4 + 1.13X_3X_4 - 4.28X_1^2 - 0.34X_2^2 + 1.33X_3^2 - 3.28X_4^2 \quad (2)$$

Where Y = CRD degradation rate (%), $X_1 = H_2O_2$ concentration, X_2 = pH, X_3 = goethite dosage and X_4 = illumination time, respectively. This semi-experimental expression of data included 15 statistically significant coefficients. Coefficients with a positive sign represent a synergistic effect, while coefficients with a negative sign represent an antagonistic effect among or between variables [25]. Thus, increasing H_2O_2 concentration, goethite

Table 2
Boe-Behnken Design arrangement and related responses.

Run	Actual values of parameters				Coded values of parameters				Y (CRD degradation rate %)	
	X_1	X_2	X_3	X_4	x_1	x_2	x_3	x_4	Actual[a]	Predicted[b]
1	3	5	1	6	0	−1	0	−1	74.50	75.80
2	3	7	0.5	8	0	1	−1	0	68.90	71.37
3	3	7	1	6	0	1	0	−1	63.30	63.08
4	5	6	1.5	8	1	0	1	0	97.30	97.53
5	1	6	1	6	−1	0	0	−1	46.60	46.31
6	3	6	1.5	10	0	0	1	1	89.00	89.38
7	3	6	0.5	6	0	0	−1	−1	68.10	69.33
8	3	6	1	8	0	0	0	0	80.00	80.18
9	3	6	1	8	0	0	0	0	80.20	80.18
10	1	7	1	8	−1	1	0	0	52.10	50.53
11	3	6	1.5	6	0	0	1	−1	72.40	72.89
12	3	5	1.5	8	0	−1	1	0	94.80	92.11
13	5	6	1	6	1	0	0	−1	87.20	84.69
14	3	7	1.5	8	0	1	1	0	76.00	76.04
15	1	6	0.5	8	−1	0	−1	0	57.10	55.48
16	5	6	1	10	1	0	0	1	96.70	96.77
17	1	6	1.5	8	−1	0	1	0	61.20	62.75
18	1	6	1	10	−1	0	0	1	60.40	62.69
19	3	6	0.5	10	0	0	−1	1	80.19	81.31
20	5	7	1	8	1	1	0	0	83.70	85.66
21	3	6	1	8	0	0	0	0	80.25	80.18
22	3	5	1	10	0	−1	0	1	93.40	92.23
23	5	6	0.5	8	1	0	−1	0	96.10	93.16
24	5	5	1	8	1	−1	0	0	98.50	101.68
25	1	5	1	8	−1	−1	0	0	64.70	64.35
26	3	6	1	8	0	0	0	0	80.23	80.18
27	3	5	0.5	8	0	−1	−1	0	85.40	85.14
28	3	6	1	8	0	0	0	0	80.22	80.18
29	3	7	1	10	0	1	0	1	77.80	75.11

[a] Y is the actual degradation rate (%) of CRD determined by experiment.
[b] Y is the predictive degradation rate (%) of CRD calculated according to Eq. (2) by Design Expert V.8.0.6 software.

Table 3
ANOVA test for response function Y (degradation rate of CRD).

Source	Sum of squares	Degree of freedom	Mean square	F-value	P-value
Model	5540.60	14	395.76	80.48	<0.0001
X_1	3938.56	1	3938.56	800.91	<0.0001
X_2	667.52	1	667.52	135.74	<0.0001
X_3	101.56	1	101.56	20.65	0.0005
X_4	607.62	1	607.62	123.56	<0.0001
X_1X_2	1.21	1	1.21	0.25	0.6276
X_1X_3	2.10	1	2.10	0.43	0.5238
X_1X_4	4.62	1	4.62	0.94	0.3487
X_2X_3	1.32	1	1.32	0.27	0.6121
X_2X_4	4.84	1	4.84	0.98	0.338
X_3X_4	5.09	1	5.09	1.03	0.3265
X_1^2	118.89	1	118.89	24.18	0.0002
X_2^2	0.77	1	0.77	0.16	0.6989
X_3^2	11.47	1	11.47	2.33	0.1489
X_4^2	69.89	1	69.89	14.21	0.0021
Residual	68.85	14	4.92		
Lack of Fit	68.80	10	6.88	658.42	<0.0001
Pure Error	0.04	4	0.01		

R^2 = 0.9877; R^2-Adjust = 0.9755; Adeq Precision = 34.72.

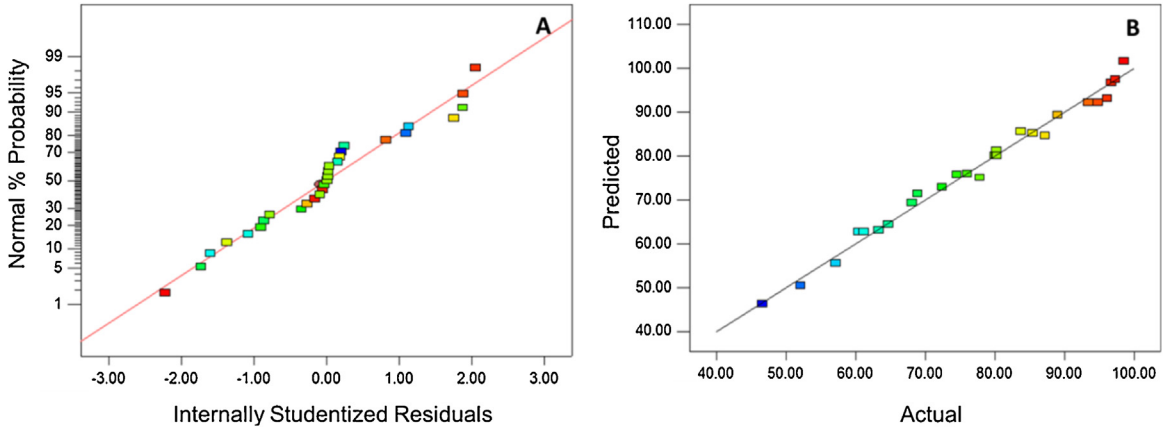

Fig. 3. Diagnostic plots of normal plot of residuals (A) and predicted versus actual values (B) for the model.

dosage and illumination time positively effect CRD degradation, while increasing pH has a negative effect. Further, the H_2O_2 concentration has a larger effect on the response than the goethite dosage and illumination time, as indicated by a larger coefficient.

Table 2 shows the combined effects of H_2O_2 concentration (X_1), pH (X_2), goethite dosage (X_3) and illumination time (X_4). Optimal reaction conditions (i.e., maximum CRD degradation, 98.50%) were as follows: H_2O_2 concentration, 4 mmol/L; solution pH, 5.0; goethite dosage, 1.2 g/L; illumination time, 9 h. Analysis of variance (ANOVA) was used to test the reliability of the model used to describe CRD removal by goethite (Table 3). All of the model variables, X_1, X_2, X_3, X_4, X_1^2 and X_4^2, were significant. The regression F-value (80.48) implies that the model is valid, as indicated by the P-value (<0.0001) [46]. The adequacy of the regression models, significance of individual model coefficients and the lack of fit were tested using the same statistical package. The P value was used to check the significance of each coefficient, necessary in turn to understand the possible interactions between variables. The larger the F-value and smaller the P-value, the higher the significance of the corresponding coefficient [47]. Based on the F-values shown in Table 3, the order of influence on CRD degradation efficiency is H_2O_2 concentration (X_1) >solution pH (X_2) >illumination time (X_4) >goethite dosage (X_3). The polynomial terms, x_1^2 and x_4^2 were significant, x_2^2 and x_3^2 were not and none of the interaction terms was significant.

The signal to noise ratio was obtained using Adeq Precision and a value >4 is desirable [47,48]. For our results, the ratio of 34.72 implies that model predictions are reliable for navigating the design space. The high regression coefficient (R^2 = 0.9877), indicates that 98.77% of the response variability is captured by

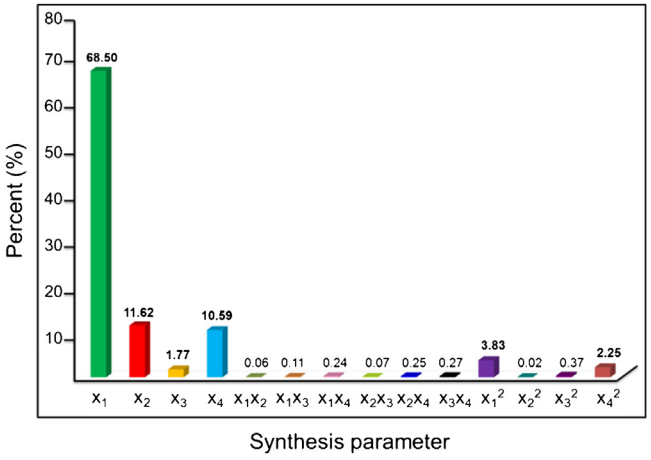

Fig. 4. Pareto graphic analysis for CRD degradation by goethite in the presence of H_2O_2.

the model [48]. The small discrepancy between R^2 (0.9877) and the adjusted R^2 (0.9755) also indicates a good fit of the model to experimental data. Fig. 3 showed the normal plot of residuals and predicted vs actual values. The close distribution of the points along the diagonal line in Fig. 3A suggests that the residuals are normally distributed and the assumption of normality was viable. Fig. 3B clearly shows the close relationship between experimental and predicted response values. These two plots demonstrate that the model is valid and reliably predicts the response to changes in the value of an independent variable [46,48].

The importance of the variables in Eq. (2) can be shown by the Pareto analysis, and the percentage effect of the single variable and the interaction variables on the response (Y) can be calculated according to Eq. (3) [25]:

$$P_i = \left(\frac{a_i^2}{\sum a_i^2}\right) \times 100 (i \neq 0) \quad (3)$$

Where P_i = effect (%) of each variable and a_i = statistically significant coefficients in Eq. (2).

Fig. 4 presents the Pareto graphical analysis of CRD degradation rate, showing that the most important parameter is H_2O_2 concentration (X_1, 68.50%), followed by solution pH (X_2, 11.62%), illumination time (X_4, 10.59%) and goethite dosage (X_3, 1.77%). The total influence of interacting variables, such as the two-factor interaction (X^2) was 6.47%.

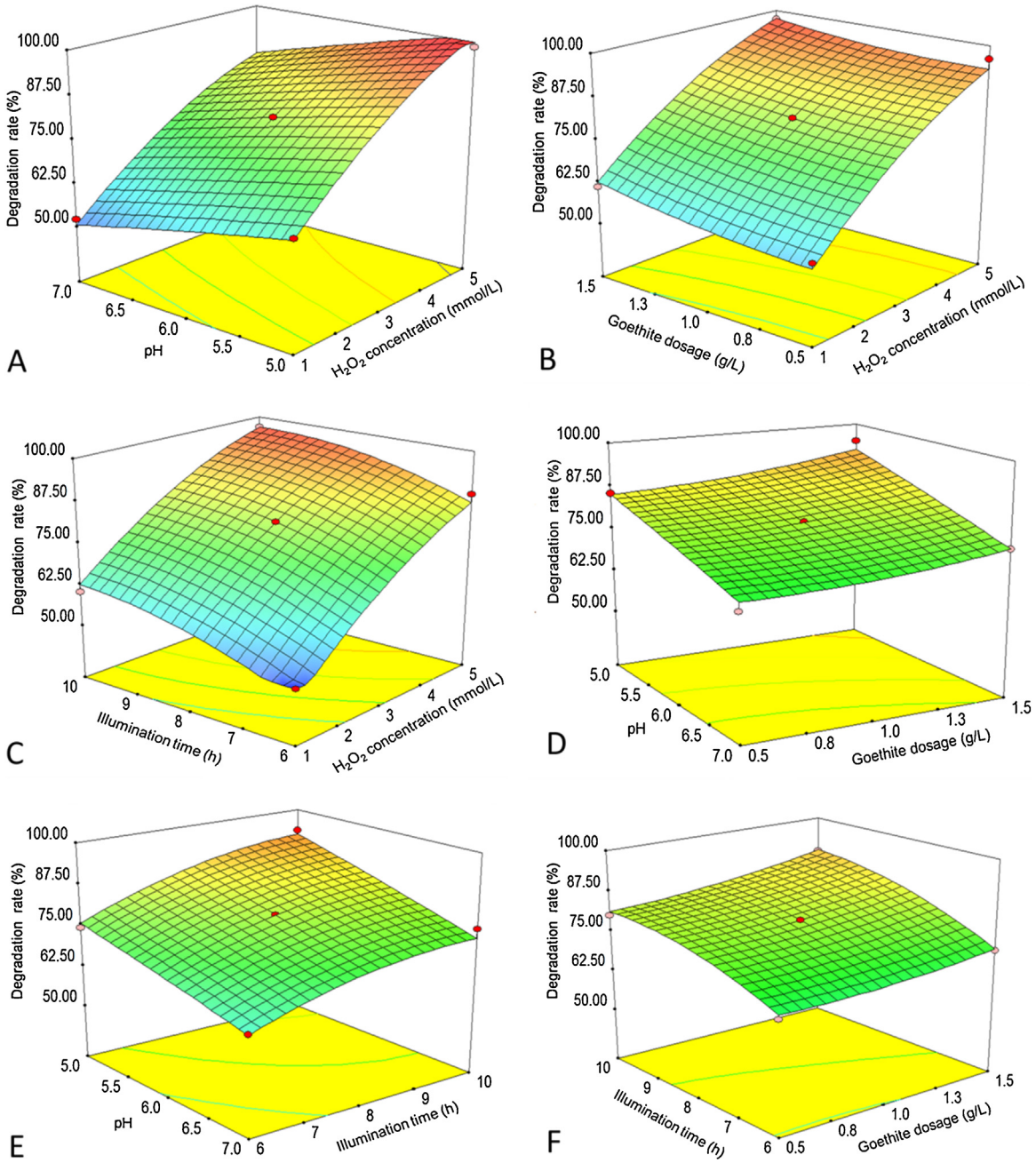

Fig. 5. 3D surface plots and contours of CRD degradation rate (%) for (A) pH vs H_2O_2 concentration, (B) goethite dosage vs H_2O_2 concentration, (C) illumination time vs H_2O_2 concentration, (D) pH vs goethite dosage, (E) pH vs illumination time, and (F) illumination time vs goethite dosage.

3D response surface plots

Three dimensional (3D) response surface plots as a function of two factors are more helpful in understanding the primary and interaction effects of the two factors [49]. The interaction effects of variables on degradation rate of CRD, within the range investigated, are visualized in the 3D plots by response surface analysis (Fig. 5). The 3D plots show that CRD degradation is favored by high H_2O_2 concentration and low pH. As can be seen in Fig. 5A–C, the degradation rate of CRD is quite sensitive to H_2O_2 concentration, indicating that H_2O_2 concentration is a critical variable in CRD photodegradation. Fig. 5A, D and E all show that an increase in pH leads to a decrease in CRD degradation. Increasing the catalyst dosage within the experimental range did not significantly effect CRD degradation (Figs. 5B, D, F) because increased catalyst dosage increases turbidity and decreases the light available for photoactivation [50]. Increasing reaction time increases the number of antibiotic molecules photodegraded, but results in diminishing returns as the reaction rate also decreases with time (Fig. 5C, E, F).

Optimization, model validation and mechanism

Optimum conditions for CRD maximum removal [Note: optimum conditions are the conditions for maximum removal, by definition] by goethite/H_2O_2 were obtained using the Design Expert V.8.0.6 software package as shown in Fig. 6. The following conditions were specified to give maximum degradation of CRD: H_2O_2 concentration, 4 mmol/L; solution pH, 5.0; goethite dosage, 1.2 g/L; illumination time, 9 h. The model output was tested by carrying out photocatalytic degradation of CRD under these conditions. CRD removal was complete (100%), as shown in the time-stepped chromatograms of CRD recorded during the confirmation experiment (Fig. 7). This result is very close to the removal extent predicted by the model (98.5%), verifying the model and its applicability to the experimental data. Fig. 7 also indicates that both the target compound and its degradation products were decomposed. The Box–Behnken Design (BBD) and response surface methodology (RSM) used in this study, known to improve research efficiency, was here shown to be a valid method for analyzing, simulating and optimizing photocatalytic degradation of pollutants.

To confirm that H_2O_2 is the primary factor affecting CRD removal, three additional degradation trials were run under optimal conditions for comparison with the complete system (Light/CRD/H_2O_2/Goet); (1) No H_2O_2 (Light/CRD/Goet), (2) no goethite catalyst (Light/CRD/H_2O_2), (3) no light (Dark/CRD/H_2O_2/Goet). The results are

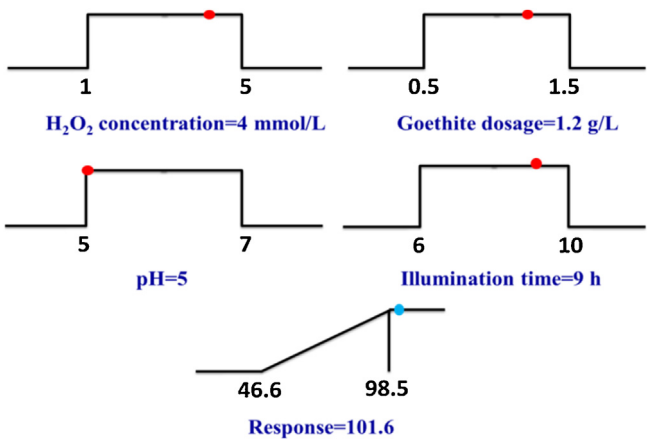

Fig. 6. Desirability ramp for numerical optimization of four independent variables, H_2O_2 concentraion, goethite dosage, pH, and illumination time.

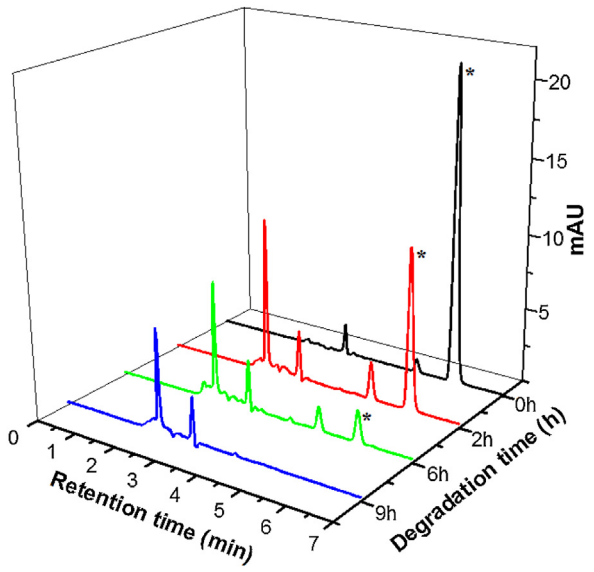

Fig. 7. HPLC graphs of CRD during the photodegradation process by goethite under the optimum conditions. (*denotes CRD peak).

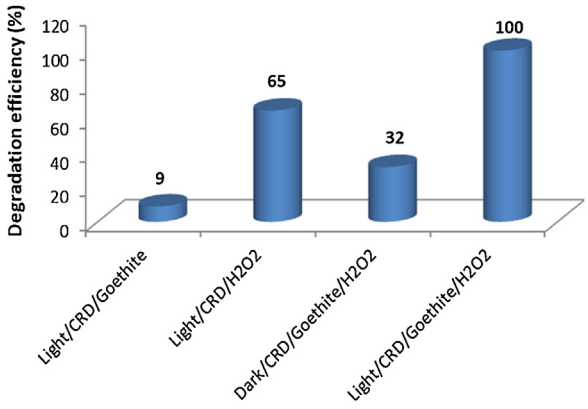

Fig. 8. Comparison of CRD degradation efficiency under different conditions.

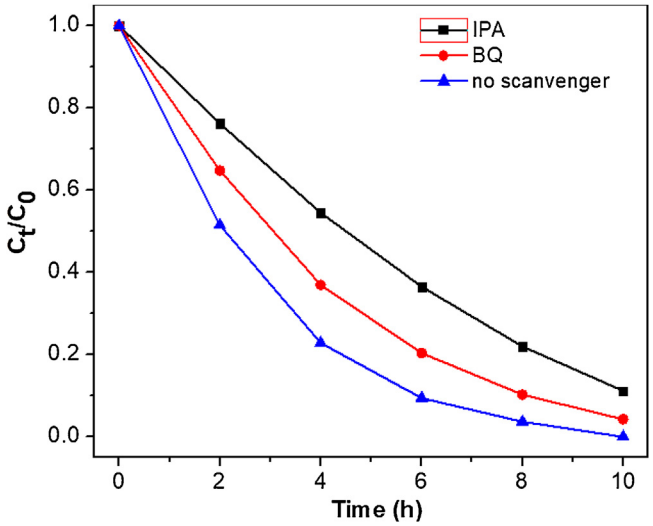

Fig. 9. Effects of various scavengers on the photocatalytic degradation of CRD by goethite.

displayed in Fig. 8. Photocatalytic degradation of CRD without H_2O_2 (9%) was much lower than with light-assisted H_2O_2 oxidation (65%) and degradation in the dark (32%) compared to photodegradation under light (100%) shows the importance of photoactivation. These results prove that H_2O_2 plays a key role in the degradation of CRD by goethite. The degradation mechanism is complex as both oxidation and photocatalysis are involved [27]. H_2O_2 may act as an electron acceptor to suppress electron–hole recombination, but can also decompose to generate the hydroxyl radical [51]. The primary reactive oxygen species (ROS) during photocatalysis was identified using selective scavengers: isopropanol (IPA) to scavenge the hydroxyl radical ($^{\bullet}OH$) and benzoquinone (BQ) to scavenge the superoxide radical ($O_2^{\bullet-}$). The results, shown in Fig. 9, show clearly that CRD degradation is inhibited by BQ and even more by IPA, indicating that both $^{\bullet}OH$ and $O_2^{\bullet-}$ are involved in photodegradation and that $^{\bullet}OH$ contributes more than $O_2^{\bullet-}$. However, the E_{CB} (+0.79 V vs. NHE) of goethite is more positive than the reduction potential of O_2 ($E^{\circ}(O_2/O_2^{\bullet-})$ = –0.33 V vs NHE) [52]. Oxygen cannot react with conduction band electrons and $O_2^{\bullet-}$ may be generated from the reaction of dissolved O_2 with Fe^{2+}, produced in small quantities from goethite.

Conclusions

In this paper, the goethite/H_2O_2 system was used to photocatalytically remove CRD from aqueous solutions. Software-assisted experimental design using Box–Behnken Design with RSM was used to determine optimal photodegradation conditions. Degradation data was fit to a second order polynomial and used to model the process, optimize reaction parameters and predict the maximum degradation extent. Optimal conditions were H_2O_2, 4 mmol/L; pH, 5.0; goethite dosage, 1.2 g/L and illumination time, 9 h with a predicted CRD degradation extent of 98.50%. Based on the P-values given by ANOVA for the RSM data, the most important factor for CRD removal was H_2O_2 concentration and the least important factor was goethite dosage. Pareto analysis indicated that H_2O_2 concentration contributed 68.5% to CRD removal. In addition, a satisfactory goodness-of-fit was observed between the predictive and experimental results, and both $^{\bullet}OH$ and $O_2^{\bullet-}$ played a role in CRD removal. This research shows the potential of a green photocatalytic system for CRD removal, the efficacy of software assisted BBD/RSM design and analysis, and contributes to a better understanding of the role that goethite plays in the transport (adsorption) and fate (photochemical oxidation) of cephalosporin antibiotics in the environment.

Acknowledgments

This work supported by the National Natural Science Foundation of China (No.21577077, 21677086, 21577078), the Innovation Group Project of Hubei province, China (No.2015CFA021) and China Postdoctoral Science Foundation Grant (No.2018M640721). We also thank Professor David Johnson, Ferrum College who helped to improve the language of the paper.

References

[1] R. Fernandes, P. Amador, C. Prudêncio, Rev. Med. Microbiol. 24 (2013) 7.
[2] A.R. Ribeiro, B. Sures, T.C. Schmidt, Environ. Pollut. 241 (2018) 1153.
[3] O. Cardoso, J.M. Porcher, W. Sanchez, Chemosphere 115 (2014) 20.
[4] N. Gilbert, Nature 481 (2012) 125.
[5] J. Zhang, J. Meng, Y. Li, C. Hu, Arch. Pharm. 343 (2010) 553.
[6] R. Guo, W. Xie, J. Chen, Food Chem. Toxicol. 78 (2015) 116.
[7] X.H. Wang, A.Y. Lin, Environ. Sci. Technol. 46 (2012) 12417.
[8] A.R. Ribeiro, B. Sures, T.C. Schmidt, Sci. Total Environ. 619–620 (2018) 866.
[9] Nature 492 (2012) 314.
[10] C.W. Knapp, J. Dolfing, P.A.I. Ehlert, D.W. Graham, Environ. Sci. Technol. 44 (2010) 580.
[11] J. Cha, K.H. Carlson, Sci. Total Environ. 640–641 (2018) 1346.
[12] L. Li, D. Wei, G. Wei, Y. Du, J. Hazard. Mater. 262 (2013) 48.
[13] M.C. Dodd, D. Rentsch, H.P. Singer, H.-P.E. Kohler, Uv. Gunten, Environ. Sci. Technol. 44 (2010) 5940.
[14] S. Navalon, M. Alvaro, H. Garcia, Water Res. 42 (2008) 1935.
[15] L. Li, D. Wei, G. Wei, Y. Du, Chemosphere 149 (2016) 279.
[16] A. Karlesa, G.A.D. De Vera, M.C. Dodd, J. Park, M.P.B. Espino, Y. Lee, Environ. Sci. Technol. 48 (2014) 10380.
[17] K. Zhang, X. Zhou, P. Du, T. Zhang, M. Cai, P. Sun, C.H. Huang, Water Res. 123 (2017) 153.
[18] J.W. Peterson, T.A. O'Meara, M.D. Seymour, W. Wang, B. Gu, Environ. Pollut. 157 (2009) 1849.
[19] A. Fakhri, S. Adami, J. Taiwan Inst. Chem. Eng. 45 (2014) 1001.
[20] H. Liu, W. Liu, J. Zhang, C. Zhang, L. Ren, Y. Li, J. Hazard. Mater. 185 (2011) 1528.
[21] D. Fabbri, M. Minella, V. Maurino, C. Minero, D. Vione, Chemosphere 134 (2015) 452.
[22] X. He, S.P. Mezyk, I. Michael, D. Fatta-Kassinos, D.D. Dionysiou, J. Hazard. Mater. 279 (2014) 375.
[23] E.A. Serna-Galvis, F. Ferraro, J. Silva-Agredo, R.A. Torres-Palma, Water Res. 122 (2017) 128.
[24] N.M. Shooshtari, M.M. Ghazi, Chem. Eng. J. 315 (2017) 527.
[25] J. Chen, J. Shu, Z. Anqi, H. Juyuan, Z. Yan, J. Chen, Diam. Relat. Mater. 70 (2016) 137.
[26] P. Bansal, A. Verma, J. Photochem. Photobiol. A 342 (2017) 131.
[27] S. Anandan, N. Pugazhenthiran, G.-J. Lee, J.J. Wu, J. Mol. Catal. A 379 (2013) 112.
[28] Y.Y. Gurkan, N. Turkten, A. Hatipoglu, Z. Cinar, Chem. Eng. J. 184 (2012) 113.
[29] Y. Xiao, X. Song, Z. Liu, R. Li, X. Zhao, Y. Huang, J. Ind. Eng. Chem. 45 (2017) 248.
[30] C. Gadipelly, A. Pérez-González, G.D. Yadav, I. Ortiz, R. Ibáñez, V.K. Rathod, K.V. Marathe, Ind. Eng. Chem. Res. 53 (2014) 11571.
[31] N. Wang, T. Zheng, G. Zhang, P. Wang, J. Environ. Chem. Eng. 4 (2016) 762.
[32] G. Boczkaj, A. Fernandes, Chem. Eng. J. 320 (2017) 608.
[33] H. Liu, T. Chen, R.L. Frost, Chemosphere 103 (2014) 1.
[34] J. He, X. Yang, B. Men, D. Wang, J. Environ. Sci. 39 (2016) 97.
[35] Y. Wang, Y. Gao, L. Chen, H. Zhang, Catal. Today 252 (2015) 107.
[36] X. Li, Y. Huang, C. Li, J. Shen, Y. Deng, Chem. Eng. J. 260 (2015) 28.
[37] R. Chen, L. Yang, Y. Guo, W. Zheng, H. Liu, Y. Wei, J. Photochem. Photobiol. A 353 (2018) 337.
[38] M. Benacherine, N. Debbache, I. Ghoul, Y. Mameri, J. Photochem. Photobiol. A 335 (2017) 70.
[39] Y. Mameri, N. Debbache, Mem. Benacherine, N. Seraghni, T. Sehili, J. Photochem. Photobiol. A 315 (2016) 129.
[40] E.G. Garrido-Ramírez, B.K.G. Theng, M.L. Mora, Appl. Clay Sci. 47 (2010) 182.
[41] Y. Ding, J. Zheng, X. Xia, T. Ren, J. Kan, Food Sci. Technol. 67 (2016) 206.
[42] C. Ai, D. Zhou, Q. Wang, X. Shao, Y. Lei, Sol. Energy 113 (2015) 34.
[43] V. Kumar Gupta, S. Agarwal, M. Asif, A. Fakhri, N. Sadeghi, J. Colloid Interface Sci. 497 (2017) 193.
[44] K.A. Caprile, J. Vet. Pharmacol. Ther. 11 (1988) 1.
[45] J.Q. Chen, R.X. Guo, J. Hazard. Mater. 209–210 (2012) 520.
[46] M. Ge, N. Zhu, Y. Zhao, J. Li, L. Liu, Ind. Eng. Chem. Res. 51 (2012) 5167.
[47] S.-L. Wang, L.-L. Wang, W.-H. Ma, D.M. Johnson, Y.-F. Fang, M.-K. Jia, Y.-P. Huang, Chem. Eng. J. 259 (2015) 410.
[48] T.Y. Ooi, E.L. Yong, M.F.M. Din, S. Rezania, E. Aminudin, S. Chelliapan, A. Abdul Rahman, J. Park, J. Environ. Manage. 228 (2018) 13.
[49] H. Bahrami, A. Eslami, R. Nabizadeh, A. Mohseni-Bandpi, A. Asadi, M. Sillanpää, J. Clean. Prod. 198 (2018) 1210.
[50] B. Iurascu, I. Siminiceanu, D. Vione, M.A. Vicente, A. Gil, Water Res. 43 (2009) 1313.
[51] H. Duan, Y. Liu, X. Yin, J. Bai, J. Qi, Chem. Eng. J. 283 (2016) 873.
[52] M. Miyauchi, Phys. Chem. Chem. Phys. 10 (2008) 6258.